

Pyramidal Search of Maximum Coherence Direction for Biomedical Image Interpolation

Jingdan Zhang*
Computer Science & Technology
Tsinghua University
Beijing 100084, P. R. China
ZhangJingdan@263.net

Yongmei Wang
Dept. of Information Engineering
The Chinese University of Hong Kong
Shatin, N. T., Hong Kong
ymwang@ie.cuhk.edu.hk

Baining Guo
Microsoft Research Asia
5F Sigma Center
Beijing 100080, P. R. China
bainguo@microsoft.com

Abstract

A multiresolution technique for biomedical image interpolation is presented in this paper. It is an extension of the work on Directional Coherence Interpolation (DCI) [15] – a novel gray-level image interpolation method that interpolates the missing image data along the smoothed Maximum Coherence Directions (MCDs). We propose to apply a pyramidal search strategy for MCD estimation. This coarse-to-fine scheme requires less computation time by starting with the reduced amount of data and propagating searching results to finer resolutions. In addition, it also improves robustness compared with our previous single resolution DCI.

1. Introduction

Multiresolution processing is a powerful idea [10, 1], whose birth is motivated by human perception. The basic principle is to first build an image pyramid. The procedure of image processing or analysis is then performed from the coarsest level to the finest level that corresponds to the image itself. There are numerous applications of this concept in the literature, such as for medical image analysis [13, 7, 11, 14], texture synthesis [3], and wavelet transform [6], etc. In this work, we apply the similar principle into 3D image interpolation problem.

Most 3D biomedical volume images are sampled anisotropically, with the distance between consecutive slices significantly greater than the in-plane pixel size. Either prior to display and measurement or during these manipulations, the volume image must be interpolated to isotropic dimensions in order to achieve the desired quality for quantitative analysis and/or visualization [9, 5]. The traditional linear interpolation scheme for 3D volume image will result in poor approximations when the distance between consecutive slices is more than five times the in-plane pixel size. The prior requirement of specific structure identification (segmentation) before interpolation limits the usefulness of the shape-based interpolation for binary images [8, 4]. To circumvent the segmenting process, a generalization of the binary shape-based method to gray-level data has been proposed [2]. However, this method is extremely time-consuming due to the computation of a high dimensional distance transform.

In order to pursue a high visual quality gray-level interpolation with modest computation cost, a new method

called Directional Coherence Interpolation (DCI) was presented in [15]. It interpolates missing image data along the smoothed Maximum Coherence Directions (MCD) between image slices instead of the coordinate axes as that in linear interpolation. By this scheme, the object structure information is well preserved without explicit representation of object boundary / surface (segmentation).

In this work, we propose a multiresolution scheme for MCD search to further reduce the computation cost and augment the interpolation accuracy of DCI.

2. Algorithm

The basis of our DCI is a form of image-space coherence [12]. The 3D form of this type of coherence, called directional coherence, is introduced and utilized into image interpolation in [15].

2.1 Single Resolution DCI (SR-DCI)

Given a 3D image, we first divide the volume space between two consecutive slices with spacing k into small cubes with size $k \times k \times k$, as shown in Figure 1(a), so that most cubes are crossed by no more than one discontinuity surface patch. Since the cube is sufficiently small, the surface patch can be regarded as flat.

The Maximum Coherence Direction (MCD), as shown in Figure 1(b), forms an integrated approach to extract discontinuity from image data, and then provides us the important image shape and structure information for interpolation. The smooth directional coherence map that describes the coherence direction over the full space between the two slices can be calculated by [15]:

$$\bar{n}^* = \arg \min_{\bar{n}} F = \arg \min_{\bar{n}} [d(\bar{n}) + \lambda \cdot s(\bar{n})] \quad (1)$$

where \bar{n}^* is the argument - smoothed MCD - that minimizes $F \forall \bar{n}$; λ is a weighting coefficient of the smoothness constraint $s(\bar{n})$ that the MCDs for adjacent cubes between the two slices change smoothly; $d(\bar{n})$ is the directional discrepancy given by

$$d(\bar{n}) = \frac{1}{A} \int_A (f(\bar{u} + t(\bar{u})\bar{n}) - f(\bar{u}))^2 ds \quad (2)$$

where S is the boundary surface of cube C_k and A is a normalization constant. For a given direction \bar{n} and a point \bar{u} on S , the scalar $t(\bar{u})$ is chosen such that the parametric line $\bar{v}(t) = \bar{u} + t(\bar{u})\bar{n}$ intersects the boundary surface S of C_k at \bar{u} and $\bar{v}(t) = \bar{u} + t(\bar{u})\bar{n}$ (Figure 1(b)). Once the intensity function $f(\bar{u})$ is known on S through surface evaluation, $d(\bar{n})$ is then a well-defined function of the direction \bar{n} . Also, we define the smoothness term as

$$s(\bar{n}) = \sum_{j=1}^P \|\bar{n} - \bar{n}_j\| \quad (3)$$

where P is the number of used neighboring local MCDs.

Given the smoothed MCD for each cube, the intensity value of a point within this cube is interpolated linearly from the values of points with known intensities along this MCD.

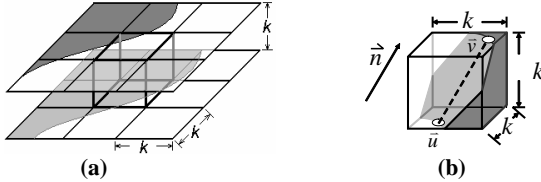


Figure 1: Diagram of (a) our volume space partition scheme between two slices (Note: the dark area denotes the existence of object / structure); (b) MCD \bar{n} for a small cube C_k .

2.2 Multiresolution DCI (MR-DCI)

2.2.1 Motivation

In general, the single resolution algorithm described above works well. However, SR-DCI has following drawbacks: i) An iterative process is employed to calculate the smoothed MCDs. In every iteration, we must exhaustively search each cube's all possible directions to determine the value of Eq.(1). Because the direction range for each cube must be large enough to obtain the correct MCDs, the executive search process is quite time-consuming. ii) When the distance between two existing slices is large, the cube's size also becomes large, the discontinuity characteristics of each cube can not be well approximated by the estimated MCD, which will therefore affect the final interpolation quality.

These problems can be solved by using a multiresolution pyramid which can represent large scale structures more compactly by a few pixels in a certain lower resolution pyramid level. The two key benefits of this technique are: First, it decreases the computation cost because most iterations are spent in processing reduced versions of the image data. Second, it usually also improves the algorithm accuracy, since the pyramid has a smoothing effect on the criterion to be optimized which often minimizes the likelihood of being trapped by local optima [10, 1].

2.2.2 Pyramidal Search Scheme for MCDs

A Gaussian pyramid is first constructed from each existing slice image by using a low-pass down-sampling operation [1]. The pyramid image, $G_i(I)$, at level i , for image slice I , is given by:

$$G_i(I) = 2 \downarrow [G_{i-1}(I) \otimes g] \quad (4)$$

where $2 \downarrow [\bullet]$ is the $2 \times$ down-sampling operation; g is a two dimensional Gaussian kernel; and $G_0(I) = I$, the original image slice. In this way, image resolution decreases by a factor of $1/2$ after each operation in Eq. (4). In implementation, we empirically utilize 3 levels of Gaussian pyramid.

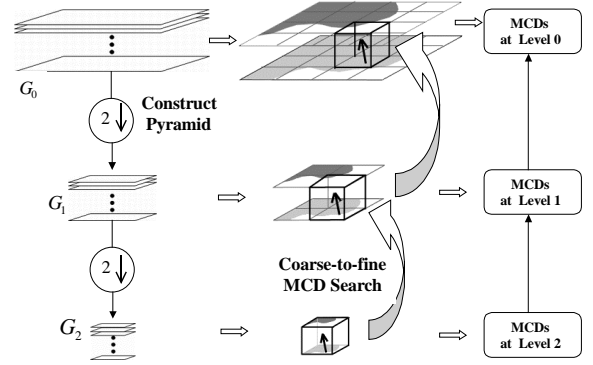


Figure 2: Coarse-to-fine flow diagram of 3-level MR-DCI. (The highlighted cube is an elementary cube at each search level, with the arrow inside representing its MCD.)

After constructing an image pyramid, we start applying the MCD search at the coarsest resolution on a small version of the image. Upon convergence, the solution is propagated to the next finer resolution where it is used as the starting condition. For each slice pair at each pyramid level G_i , the smoothed MCDs are calculated in a way similar as that for the single resolution case with the following modifications: At each level, the initial MCD value and the direction search range for every cube are determined based on the respective resolution level. Specifically, at the coarsest level (Level 2 in Figure 2), the initial MCD of the cube is set to be vertical to the cube's top and bottom facets. For the other fine levels (Level 1 and Level 0), the initial MCD of the cube is obtained through bilinear interpolation of the MCDs that are already calculated in the previous lower resolutions (corresponding Level 2 and Level 1, respectively). A hidden condition during the search is that the length of the cubes at all levels is the same. As to the direction search range, at the coarsest level, the range must be large enough to cover all the possible directions; whereas at finer levels, this range can be gradually decreased since the major aim of the fine-scale search is to refine the MCDs estimated from the previous coarser level. This type of coarse-to-fine iteration strategy is proceeded until the finest level of the pyramid (Level 0) that corresponds to the image itself is reached.

2.2.3 Point-wise MCD Computation

At this stage of the process, the MCDs are cube-based. That is, all points within one cube only have one MCD. In order to assign a MCD for every point and ensure the neighboring points' MCDs vary smoothly, we employ a bilinear interpolation of MCDs. The detailed technique is shown in Figure 3.

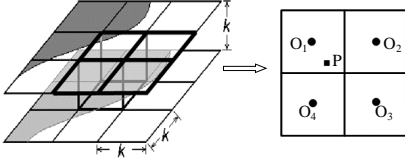


Figure 3: Diagram of point-wise MCD computation. (O₁, O₂, O₃, and O₄ represent the center points of 4 nearby cubes; their MCDs are defined as the respective cubes' estimated ones. The MCD for an arbitrary point, P, is calculated through bilinear interpolation of the 4 nearby center points' MCDs.)

2.2.4 Gray-level Interpolation along MCDs

Given the smoothed MCD for each voxel, the gray-level value of the "new voxel" is then interpolated linearly from the values of points with known values along its individual MCD. Refinement scheme is applied to interpolate the images to the desired scale. An isotropic 3D image with well preserved structure is then generated when the whole process in Section 2.2 is repeated for all the slice pairs.

3. Experiments and Results

For all the experiments, we have compared the proposed multiresolution directional coherence interpolation (MR-DCI) with the traditional linear interpolation (LI), shape-based interpolation applicable to gray level images (SBI) [2], and our previous single resolution DCI (SR-DCI) [15].

3.1 Synthetic Image Pair

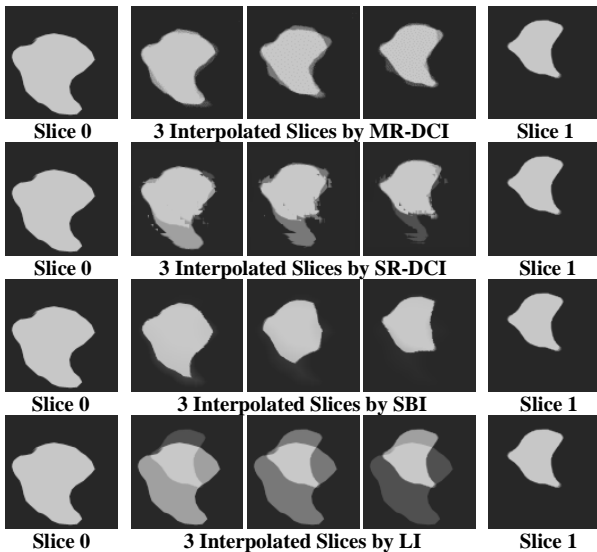


Figure 4: Comparison experiment on synthetic image pair.

The experiment in Figure 4 demonstrates the robustness of MR-DCI. The left and right columns are the original slice pair (Slice 1 is a rotated, translated and scaled version of Slice 0). Different rows of the middle three columns correspond to the interpolated slices by the four methods. We can see that the object structure / shape is well preserved in MR-DCI by using a coarse-to-fine search strategy. Due to the large difference between the two existing slices, MCD search at single resolution is not as robust as the pyramidal search of MCD. The interpolated slices by SBI and LI are also not reasonable.

3.2 3D MR Brain Image

We have applied the four methods to real MR scan of a human brain (image size 256x256x167). The test image is generated by dropping the slices between every 4 and 8 slices from the original volume data. We need to interpolate 3 and 7 slices for the generated data so that the interpolated volume image is recovered to the same size as the original one. The dropped slices are then used as the ground truth for validation.

3.2.1 Rendering Effects

An important advantage of our DCI method is that it leads to good 3D volume rendering effects in visualization [15], which can be seen in Figure 5, too. The rendered image from the original true data is also available for comparison. The 3D rendering results from SR-DCI and MR-DCI are similar (with MR-DCI a little better - smoother), but they are substantially improved compared with those from LI, where there are severe jagged staircase artifacts. SBI gives better rendering quality than LI, but not as good as our two DCI methods.

3.2.2 Error Measures

To evaluate the methodology quantitatively, we use the four error measures computed between the original true data and the interpolated data, as in [15]:

- $E_a = \sqrt{\text{Mean squared difference in Intensity}}$
- $E_b = \sqrt{\text{Opacity} \cdot \text{Mean squared difference in Intensity}}$
- $E_c = \sqrt{\text{Opacity} \cdot \text{Mean squared difference in Gradient}}$
- $E_d = \sqrt{\text{Opacity} \cdot \text{Mean squared difference in Opacity}}$

The mentioned error measures for the MR brain are shown in Table 1. Almost all the error measures from our MR-DCI are the best among the four methods, although the improvement in some cases is limited.

3.2.3 Computation Time

The four methods' approximate execution times on a PC (Pentium III 866Mhz 256MB RAM) are also listed in Table 1 for comparison. Although SR-DCI takes longer time than the simple LI, it is significantly faster than the shape-based scheme applied on gray-level images. Moreover, compared with SR-DCI, MR-DCI can further reduce the computation cost due to the pyramidal search of MCDs.

Measures	Slice Spacing	MR-DCI	SR-DCI	SBI	LI
<i>Ea</i>	4	4.01	4.09	4.19	4.22
	8	6.12	6.41	6.24	6.43
<i>Eb</i>	4	3.64	3.71	3.87	3.81
	8	5.48	5.70	5.73	5.68
<i>Ec</i>	4	2.39	2.38	2.54	2.52
	8	3.21	3.30	3.45	3.40
<i>Ed</i>	4	0.192	0.194	0.204	0.193
	8	0.232	0.235	0.244	0.232
Comp. Time	4	1.432	4.762	99.09	0.040
	8	1.374	3.766	64.47	0.040

Table 1: Quantitative comparison of error measures (pixels) and computation time (minutes) on MR brain volume image.

4. Conclusions

A multiresolution Direction Coherence Interpolation method (MR-DCI) is presented in this paper. It interpolates the intensity values of “new voxels” along their smoothed Maximum Coherence Directions (MCDs), which are estimated by using a pyramidal search algorithm. Experiments on both synthetic and real biomedical data show that in addition of the principal advantages reported in our previous work, the proposed MR-DCI can further decrease the computation time and augment the interpolation robustness.

Acknowledgements

The second author is supported in part by the Research Grants Council of the Hong Kong SAR, under RGC Earmarked Grant (Project No. CUHK 4195/01E), and under Direct Grant for Research (Project Code: 2050258).

* The first author participated in this work when he was working as an intern at Microsoft Research Asia.

References

[1] P. J. Burt and E. H. Adelson, “A multiresolution spline with application to image mosaics”, *ACM Trans. Graphics*, 2(4), pp. 217-236, 1983.

[2] G. J. Grevera and J. K. Udupa, “Shape-based interpolation of multidimensional gray-level images”, *IEEE Trans Medical Imaging*, 15(6), pp. 881-892, 1996.

[3] D. J. Heeger and J. R. Bergen, “Pyramid-based texture analysis/synthesis”, *Proc. SIGGRAPH’95*, pp. 229–238, 1995.

[4] G. T. Herman, J. Zheng and C. A. Bucholtz, “Shape-based interpolation”, *IEEE Computer Graphics and Applications*, 12(3), pp. 69-79, 1992.

[5] T. M. Lehmann, Claudia Gonner and K. Spitzer, “Survey: Interpolation methods in medical image processing”, *IEEE Trans. Medical Imaging*, 18(11), pp. 1049-1075, 1999.

[6] S. G. Mallat, “A theory of multiresolution singla decomposition: the wavelet representation”, *IEEE Trans. Pattern Anal. and Machine Intell.*, 11, pp. 674-693, 1989.

[7] S. M. Pizer, D. S. Fritsch, P. A. Yushkevich, V. E. Johnson, and E. L. Chaney, “Segmentation, registration, and measurement of shape variation via image object shape”, *IEEE Trans. Medical Imaging*, 18(10), pp. 851-865, 1999.

[8] S. P. Raya and J. K. Udupa, “Shape-based interpolation of multidimensional objects”, *IEEE Trans. Medical Imaging*, 9(1), pp. 32-42, 1990.

[9] R. A. Robb, *Biomedical Imaging, Visualization, and Analysis*, Wiley-Liss, Inc., 2000.

[10] A. Rosenfeld, *Multiresolution Image Processing*, Berlin, Germany: Springer-Verlag, 1984.

[11] D. Shen, E. H. Herskovits, and C. Davatzikos, “An adaptive focus statistical shape model for segmentation and shape modeling of 3-D brain structures”, *IEEE Trans. Medical Imaging*, 20(4), pp. 257-270, 2001.

[12] L. Sutherland, R. Sproull and R. Schumacker, “A characterization of ten hidden-surface algorithms”, *ACM Computing Surveys*, 6(1), pp.387-442, March 1974.

[13] P. Thevenaz, M. Unser, “Optimization of mutual information for multiresolution image registration”, *IEEE Trans. Image Processing*, 9(12), pp. 2083-2099, 2000.

[14] Y. Wang, B. S. Peterson, and L. H. Staib, “Shape-based 3D surface correspondence using geodesics and local geometry”, *IEEE Conf. Computer Vision and Pattern Recognition*, pp. 644-651 (vol. II), June 2000.

[15] Y. Wang, Z. Zhang and B. Guo, “3D image interpolation based on directional coherence”, *IEEE Workshop on Mathematical Methods in Biomedical Image Analysis*, pp. 195-202, Hawaii, December 2001.

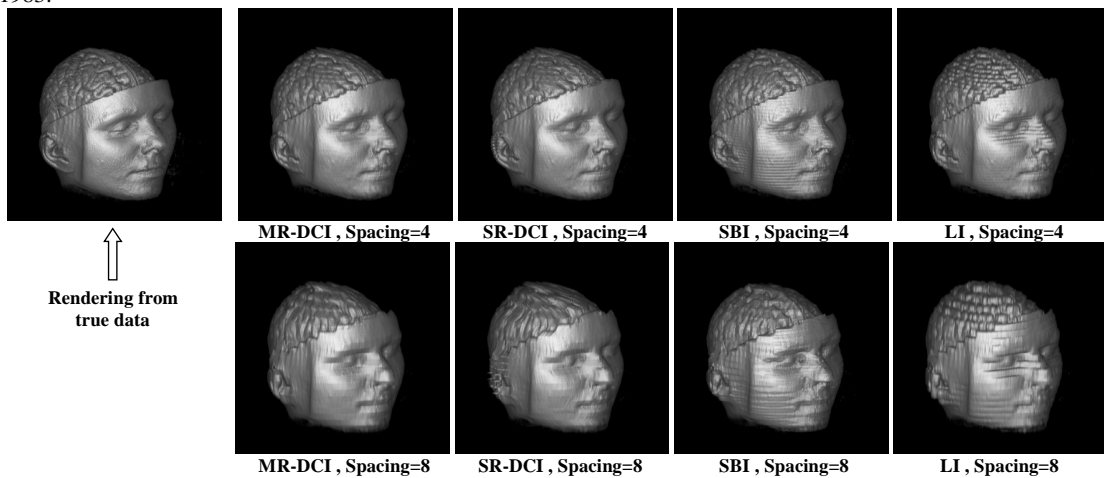


Figure 5: Comparison of 3D volume rendering on MR brain.